Concepts, Instruments, and Model Systems that Enabled the Rapid Evolution of Surface Science

Gabor A. Somorjai [1, 2,]* and Jeong Y. Park[1, 2]

[1]*Department of Chemistry, University of California, Berkeley, CA 94720*

[2]*Materials Sciences Division and Chemical Sciences Division, Lawrence Berkeley National Laboratory, Berkeley, CA 94720*

Abstract

Over the past forty years, surface science has evolved to become both an atomic scale and a molecular scale science. Gerhard Ertl's group has made major contributions in the field of molecular scale surface science, focusing on vacuum studies of adsorption chemistry on single crystal surfaces. In this review, we outline three important aspects that led to the recent advances of surface chemistry: the development of concepts, *in situ* instruments for molecular scale surface studies at buried interfaces (solid-gas and solid-liquid), and new model nanoparticle surface systems in addition to single crystals. Combined molecular beam surface scattering and low energy electron diffraction (LEED)- surface structure studies on metal single crystal surfaces revealed new concepts, including adsorbate-induced surface restructuring and the unique activity of defects, atomic steps and kinks on metal surfaces. We have combined high pressure catalytic reaction studies with ultrahigh vacuum (UHV) surface characterization techniques using the UHV chamber equipped with a high-pressure reaction cell. New instruments, such as high pressure sum frequency generation (SFG) vibrational spectroscopy and scanning tunneling microscopy (STM) have been built that permit molecular-level surface studies performed at pressures. Tools that can access broad ranges of pressures can be used for both the *in situ* characterization of buried interfaces of solid-gas and solid-liquid and the study of catalytic reaction intermediates. The model systems for the study of molecular

surface chemistry have evolved from single crystals to nanoparticles in the 1-10 nm size range, which are the preferred media in catalytic reaction studies.

*To whom correspondence should be addressed. E-mail:somorjai@berkeley.edu

I. Introduction

Over the last several decades, surface science has undergone revolutionary advances that reveal on the atomic- and molecular-level structural, dynamic, compositional, and thermodynamic properties of surfaces that are utilized in chemical process development to correlate these data with adsorption and reaction rates and catalytic selectivity to deliver desired chemical properties(1-9). In this review, we highlight recent studies of three important aspects in developing instrumentation, concepts, and model systems that permitted the rapid evolution of surface science. Surface science evolved such that new instruments for surface analysis on the molecular scale could be used in a vacuum or at realistic conditions such as high pressures and at solid-liquid interfaces where the chemical processes typically operate (bridging the pressure gap) (10). Surface science also led the studies of new nanomaterials that have increased reaction rates and improved chemical selectivity (bridging the materials gap) (8; 9). Through molecular-scale investigations, new concepts were developed to understand how catalysts work at the molecular scale (11).

We provide important surface phenomena revealed by vacuum studies on single crystal surfaces in Section II. We outline the development of in-situ instruments for molecular scale surface analysis in Section III. Section IV provides the concepts uncovered by surface science studies at high pressure. We highlight the evolution of model systems from the single crystal surfaces to colloid nanoparticle systems in Section V. Finally, in Section VI, we provide future directions of surface science that include the role of hot electrons in surface chemistry and heterogeneous catalysis, and molecular adsorption at hydrophobic and hydrophilic surfaces in water that are important in the chemistry of biointerfaces.

II. Phenomena revealed by surface science studies in vacuum

Vacuum studies on single crystal surfaces revealed a number of important surface phenomena, leading to new concepts in surface science. The instrumentation techniques developed for surface studies (12) include photon-in/electron-out (X-ray photoelectron spectroscopy (XPS)), electron-in/electron-out (low energy electron diffraction (LEED) surface crystallography and Auger electron spectroscopy (AES)), atomic or molecular beams, or ion beam in/ions out (secondary ion mass spectrometry (SIMS) and inelastic ion surface scattering (ISS) techniques). All of these techniques have high scattering cross sections that would not survive the presence of high pressure gas or liquid at the interfaces. In a vacuum, or at low pressures that permit high enough mean free paths for the exiting particle surface probes to be detectable, one could determine the surface composition with less than 1% of a monolayer sensitivity, electronic structures and oxidation states of surface atoms, and the surface structures of clean surfaces and adsorbed atoms and molecules with their bond distances and bond angles (13). Usually, single crystals were used in these studies to serve as model surfaces. Figure 1 shows a photograph of a Pt(111) single crystal sample in the high pressure reactor cell ((a) in the open and (b) closed position) in the ultrahigh vacuum chamber. This chamber is equipped with LEED and AES for surface science studies in vacuum.
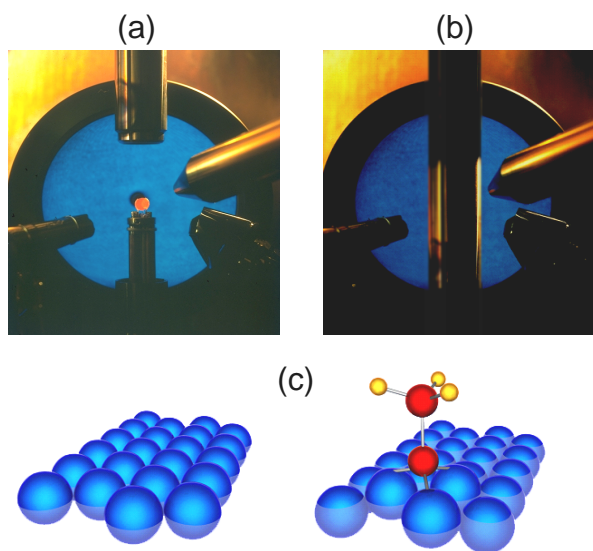

Figure 1. Photograph of UHV high-pressure cell apparatus with Pt single crystal (a) in open position and (b) in closed position. The vacuum chamber is equipped with low energy electron diffraction, Auger electron spectroscopy, and mass spectroscopy for surface science studies in vacuum. (c) Ethylidyne-induced restructuring of platinum (111) surface during ethylene hydrogenation.

Many major discoveries were made by these vacuum studies. Clean surface reconstruction of semiconductors and metals showed that surface structures are very different from structures in the bulk. This holds true for alkali halides, oxides and even ice. Adsorbed atoms and molecules occupy sites of stronger bonding on surfaces and cause further restructuring of

surface atoms (14-16). Figure 1c shows the Pt (111) single crystal surface and ethylidyne-induced surface restructuring of Pt(111) upon adsorption of ethylene. It was discovered that surfaces have defects, atomic steps (often periodic) and kinks in the steps that are chemically active, leading to the site selectivity on adsorption of molecules (17; 18) or dissociation of adsorbing molecules(19). Surface thermodynamic studies using calorimetry and thermal desorption revealed that the heat of adsorption (desorption) depends on the coverage of adsorbing molecules due to the presence of adsorbate-adsorbate interactions (20). Bimetallic or multi-component systems show surface segregation as the lower surface free energy component accumulates on the surface (21; 22). Segregation at the surface is also affected by adsorption as the chemical bonds between adsorbed atoms and the substrate change the surface composition. Molecular and atomic beam scattering studies revealed the nature of energy transfer at the surface during a single collision(23-25).

In order to demonstrate that chemical reaction studies at high pressures are essential, we focus on the chemical behavior of variou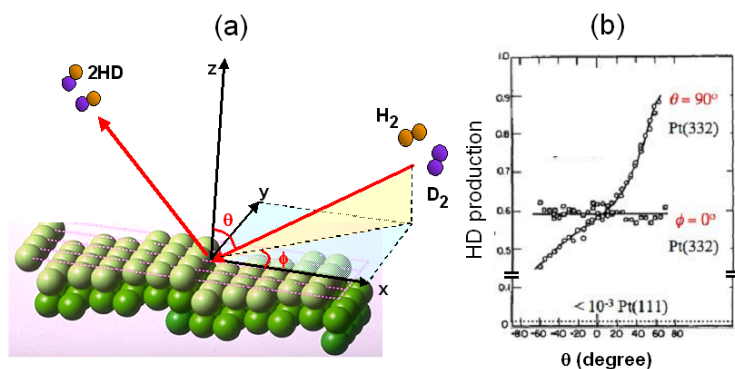s single crystal surfaces of platinum. A stepped surface exhibits unique chemical activity. When one of the simplest reactions, H_2/D_2 exchange, was investigated by molecular beam scattering the dissociation of hydrogen molecules to atoms had a reaction probability of unity -

Figure 2. Molecular beam scattering studies of H_2-D_2 exchange on Pt(332) surface, showing that atomic steps on metal surfaces break chemical bonds, in this case hydrogen-hydrogen bonds, with a reaction probability of unity. (a) schematic defining the geometry of the incident angle (polar θ and azimuthal ϕ) of the molecular beam with respect to a stepped surface. (b) HD production as a function of angle of incidence θ of the molecular beam normalized to the incident D_2 intensity. The plot was taken at the beam modulation frequency of 10 Hz and the surface temperature of 800 ^{o}C

that is, every hydrogen molecule was dissociated when scattered from the stepped platinum surface(19; 26). When a defect-free platinum (111) crystal face was prepared, the dissociation probability of molecular hydrogen was below the detection limit of 10^{-3},

as shown in Figures 2a and 2b. At elevated pressures, however, where the collision rate of H_2 molecules with the metal surface was high H_2/D_2 exchange was readily detectable even from the (111) crystal face of the metal. We consider another chemical dissociation reaction, the breaking of carbon hydrogen bonds by dissociation of methane, CH_4. When methane was incident on the Pt(111) surface the dissociation probability to produce carbon and hydrogen, which ultimately deposited a layer of carbon on the platinum surface, was below 10^{-8} (27). This type of C-H bond breaking reaction cannot be detected at low pressures or in ultra-high vacuum. We need at least 1 Torr of methane colliding continuously with the platinum single crystal surface to detect the deposition of carbon atoms within 60 seconds. Such high pressure is absolutely essential to detect the formation of CH_3 molecules, and the subsequent rearrangement to C-CH_3, C-H, and C_2H molecular segments on the surface by vibrational spectroscopy. Thus, the surface is populated by sites where reaction probabilities to break or rearrange chemical bonds vary by orders of magnitude and, to access both the active and less active sites, high reactant pressures are needed. These results demonstrate the importance of surface science studies at high pressure.

III. Development of high-pressure instruments – bridging the pressure gap

In this section, we highlight three in-situ high pressure instruments, a high pressure-ultra high vacuum combined system, sum frequency generation (SFG) vibrational spectroscopy and scanning tunneling microscopy (STM). Figure 1a shows the high-pressure cell in open position that is equipped with LEED, AES, and mass spectrometry, allowing us to study the surface composition and surface structure in vacuum. In the closed position as shown in Figure 1b, the sample surface is enclosed by the high-pressure cell and the rates of catalytic turnover at high pressures can be monitored.
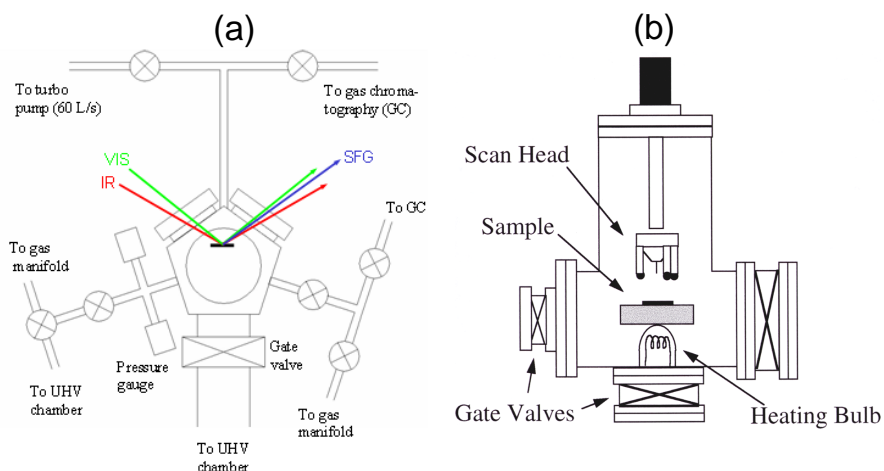
Figure 3. (a) Schematics of high pressure sum frequency generation (HP-SFG) vibrational spectroscopy and (b) high pressure scanning tunneling microscopy (HP-STM).

One of the most useful techniques for high-pressure studies is non-linear laser optics based SFG vibrational spectroscopy (Figure 3a) (3; 28-31). This is a surface specific technique that was developed in Berkeley, based on the principle of second harmonic generation (30). One or both laser frequencies are tuned and spatially and temporally overlapped. By scanning one of the lasers in the infrared frequency regime a sum frequency signal is obtained, and thus a visible vibrational spectrum. Such a signal is forbidden from a centrosymmetric medium, such as the bulk of face centered cubic crystals or an isotropic high pressure gas or a liquid. However, at the surface that is not centrosymmetric, the second order susceptibility of non-zero is allowed, and the surface yields a vibrational spectrum that is monolayer sensitive. It is also able to give vibrational frequencies of adsorbed molecules at pressure ranging through 10-12 orders of magnitude. It was found that vibrational spectra of carbon monoxide and ethylene on Pt (111) surface are virtually pressure independent for these molecules adsorbed on the metal surface (32; 33).

Another technique that can be used at equally well high pressures and in an ultra high vacuum is STM (Figure 3b).(5; 34-37). Although most researchers use this technique at low pressures, when it is used around 150 Torr one can see ordered surface structures of carbon monoxide that are not seen at low pressures. Due to the close packing of these molecules on the surface, there is an increase in repulsive interaction among molecules that leads to ordering, which is not observable at low pressures. In addition, the adsorption of various gases at high pressures often induces reconstruction of the surface due to the high coverage of strongly adsorbed atoms or molecules.

IV. Concepts of surface science at high pressures

The development of new instrumentations in high pressure has brought the concepts of surface science at high pressure, such as detection of *reaction intermediates* and *mobility of adsorbate molecules*. In this section, we focus on two chemical reactions, ethylene hydrogenation to ethane and hydrogen/deuterium exchange and its poisoning with carbon monoxide. Figure 4a shows an SFG spectrum that reveals three *reaction intermediates* of ethylene hydrogen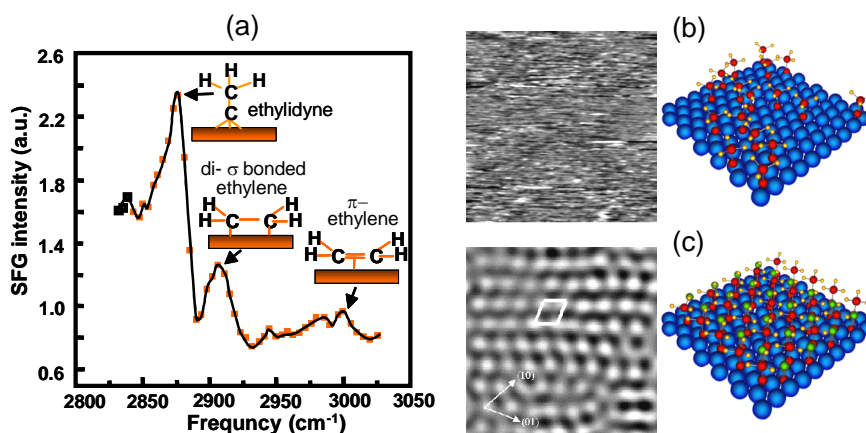ation: ethylidyne, π-bonded ethylene, and di-σ ethylene(28). By using carbon isotopes, ethylidyne was found to be a strongly adsorbed spectator that covered 96% of the platinum surface and stayed on the surface a million times longer than the turnover rate of ethylene hydrogenation.

Figure 4. (a) SFG spectrum of the Pt (111) surface during ethylene hydrogenation revealing reaction intermediates, ethylidyne, di-σ bonded ethylene, and π- ethylene. The spectrum was measured with 100 Torr of H_2, 35 Torr of C_2H_4, and 615 Torr of He at 295 K. (b) 10 nm x 10 nm STM images of Pt (111) surface at 20 mTorr H_2 and 20 mTorr C_2H_4, (c) 10 nm x 10 nm STM images of Pt (111) surface at 20 mTorr H_2, 20 mTorr C_2H_4, and 5 mTorr CO.

The study of the surface structure of ethylene reveals that π-bonded ethylene was a weakly adsorbed intermediate, as compared to di-σ ethylene and ethylidyne. Thus, it was π-bonded ethylene that turned over and formed ethane during ethylene hydrogenation.

As the surface is scanned at a speed of about 10 nm per millisecond the high pressure STM shows no structural features under ethylene hydrogenation as shown in Figure 4b(38). This indicates that the adsorbed molecules under reaction conditions are mobile on the surface, and they have a ***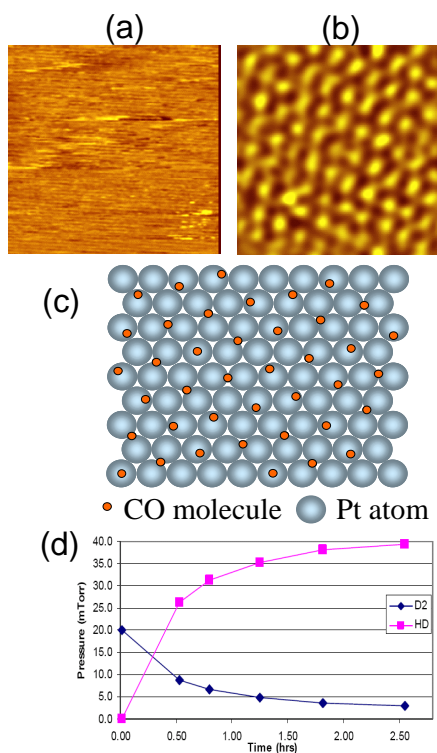mobility*** higher than the scanning rate of our STM tip. However, when we add another molecule, carbon monoxide, to the surface it acts as a poison, the reaction stops and the STM picture shows a high level of order on the surface as shown in Figure 4c. It appears that the ordering of CO prohibits the ***mobility*** of the reactants and catalysis is inhibited in several different reaction studies due to this. Using high pressure STM, we always find that the adsorbed layer is mobile in the catalytically active surface while, if the reaction is inhibited by another adsorbate that poisons the catalytic reaction, ordered structures form.

Figure 5. (a) 90 Å x 90 Å STM images of catalytically active Pt(111) at 298 K: (a) in the presence of 200 mTorr H_2 and 20 mTorr D_2. (b) in the presence of 200 mTorr H_2, 20 mTorr D_2, and 5mTorr CO. (c) CO molecules are represented by the small circles and color coded according to their proximity to a top site (dark) or to a bridge site (light). (d) D_2 and HD were monitored with mass spectroscopy at 296K, 200 mTorr H_2, and 20 mTorr D_2. The evolution of D_2 and HD partial pressure indicates that Pt catalyst surface is actively producing HD, consistent with the STM image (a).

Catalytic hydrogen/deuterium exchange on a platinum (111) single crystal and its poisoning with carbon monoxide was also studied using STM and mass spectrometry at reaction conditions at pressures ranging from mTorr to atmospheric range(39).

STM images acquired at room temperature under reaction conditions (200 mTorr H_2, 20 mTorr D_2) show a surface with no discernible order (Figure 5a) as the adsorbate species are diffusing much faster than the scanning rate of our instrument (10 nm per millisecond). STM images of the surface, after introducing 5 mTorr of CO to poison the reaction, revealed an ordered surface with

hexagonal symmetry (Figure 5b), which is similar to that formed by pure CO on Pt(111) in this pressure range. The structure is incommensurate with that of the Pt(111) lattice and has a coverage of about 0.6 monolayer. A schematic of the proposed structure is shown is Figure 5c.

It was found that at room temperature and in the presence of 200 mTorr of H_2 and 20 mTorr of D_2, the surface is catalytically active, producing HD at a rate of 4.3 molecules/site/s as shown in Fig. 5d. Upon introduction of 5 mTorr of CO, however, the production of HD dropped below the detection limits of our mass spectrometer. At 345 K, the turnover frequency in the absence of CO increased to 39 molecules/site/s, which is about 10 times higher than that at room temperature. Addition of 5 mTorr of CO at this temperature decreased the reactivity dramatically, but unlike in the room-temperature case, catalytic activity was still observed at the rate of 0.03 molecules/site/s. This implies that the immobile and ordered monolayer of CO molecules forms an incommensurate structure relative to the Pt(111) substrate. Removing a small fraction of the CO layer by heating the sample allowed the surface to become mobile and catalytically active. It was also found that the activation energy for the H_2/D_2 exchange reaction in the absence of CO is 5.3 kcal/mol. The introduction of CO into the system causes the activation energy to more than triple to 17.4 kcal/mol. The activation energy after CO poisoning was observed for ethylene hydrogenation on Pt(111), where the activation energy increased from 9.6 kcal/mol for the clean surface to 20.2 kcal/mol for the CO-poisoned surface(40; 41).

Surface science studies at high pressure also suggest that ***adsorbate-induced restructuring at high pressures*** is a more facile and more dominant phenomena. The dynamic surface under high pressure condition undergoes rapid adsorbate-induced restructuring on the time scale of chemisorption as adsorbate bonds form or break. This concept of surface science at high pressure can be applied to the emerging surface materials, such as nanoparticles. Catalysis may take place more easily in a nanoparticle form, where less atoms and molecules participate in the restructuring during the catalytic turnover.

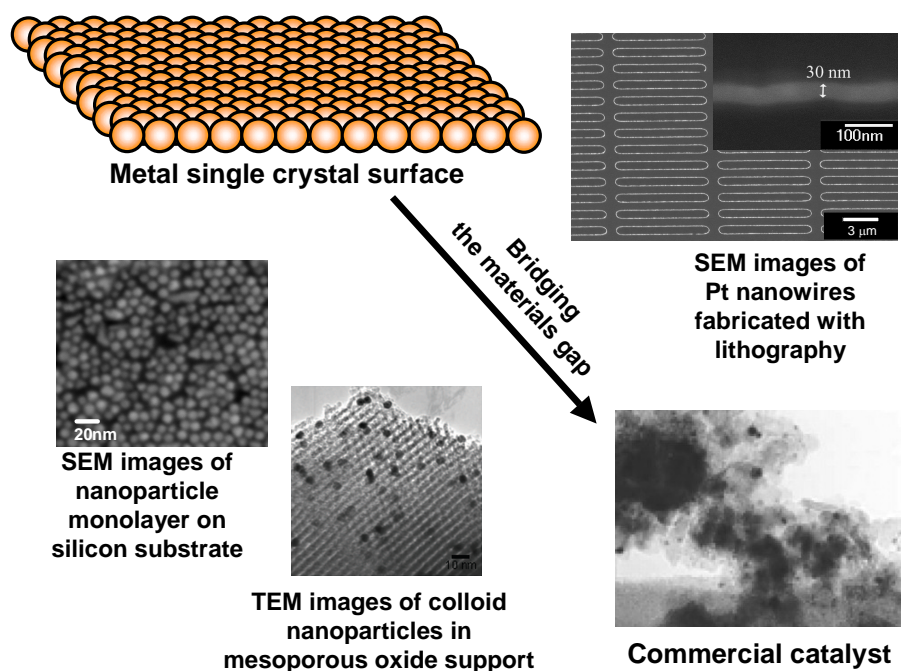**V. Development of a model system - bridging the materials gap**

Metal single crystal surface

Bridging the materials gap

30 nm

100nm

3 µm

SEM images of Pt nanowires fabricated with lithography

20nm

SEM images of nanoparticle monolayer on silicon substrate

10 nm

TEM images of colloid nanoparticles in mesoporous oxide support

Commercial catalyst

Figure 6. Schematic showing new model catalyst systems to bridge the materials gaps from a single crystal metal surface to a commercial catalyst. New model systems include two-dimensional nanoparticle arrays, colloid nanoparticles encapsulated into a mesoporous oxide support, and nanowire arrays fabricated with lithography.

Chemically active surfaces are not single crystals, but are frequently nanoparticles 1-10 nm in size. The use of single crystals as model catalytic systems has shed light on many surface concepts and phenomena, as shown in Section II and Section IV. Industrial catalysts, however, do not just consist of metal, but are made up of metal particles 1–10 nm range dispersed in a high surface area support, as shown in Figure 6. They are produced by synthesizing the metal particles and support separately and then dispersing the metal clusters onto the support by techniques such as wet-impregnation, co-precipitation, or ion-exchange. Thus, single-crystalline metals used for modeling industrial catalysis inherently lack the complexity needed to uncover many of the factors important to catalytic turnover and selectivity on nanoparticles. Considerations such as metal support interactions and the importance of metallic cluster size are of extreme importance to catalytic applications.

In order to bridge this materials gap, several new model systems have been proposed and utilized, as shown in Figure 6. The first approach involves the fabrication of Pt nanoparticle and nanowires with lithography techniques. Pt nanoparticle arrays 30 nm in size were fabricated with electron beam lithography(42), which utilizes high-resolution pattern writing and an electron-sensitive resist/etching. Disadvantages of electron beam lithography are low throughput and high cost. Thus, we utilized size reduction lithography (SRL) and nanoimprint lithography (NIL)(43; 44). Several repetitions of size reduction lithography can reduce the size of mold to ~ 7 nm silicon nanowire. The nanowire pattern is transferred into poly methylmethacrylate (PMMA) under high pressure and high temperature by using nanoimprint lithography. Then, a thermal oxide layer formed by oxygen-plasma etching on the residual PMMA is removed, with the final product being a nanoscale mold. Pt atoms can be deposited by electron beam evaporation to form Pt nanowires. Figure 4b shows the Pt nanowire arrays on a silicon oxide surface with a width of 30 nm. Thermal treatment in a vacuum, hydrogen or oxygen crystallized the Pt nanowires. Catalytic reactions including ethylene hydrogenation and CO oxidation were carried out on Pt nanowires on oxide supports(45). It was found that the turnover rate of ethylene hydrogenation is proportional to the oxide–metal periphery area, even though the nanoparticles are poisoned, suggesting the oxide-metal interface functions as a reactive site(41).

Nanoparticles are prepared by colloid synthesis, and in this circumstance they are capped with a polymer to prevent their aggregation in the solution. These can be monodispersed of uniform size and shape and can be deposited as a two-dimensional film by the Langmuir-Blodgett technique(46). The nanoparticles can also be deposited in a mesoporous three-dimensional oxide framework at much higher surface concentrations(47-50). The particle size and shape and the interface sites between the metal particles and the oxide where they are deposited are important aspects that control reaction selectivity(46; 51). The development of new model systems permit us to study phenomena associated with reduced dimensions, such as chemical activity and reaction selectivity variation due to metal nanoparticle size and shape, as well as the role of oxide-metal interfaces, which are fundamental questions in surface chemistry.
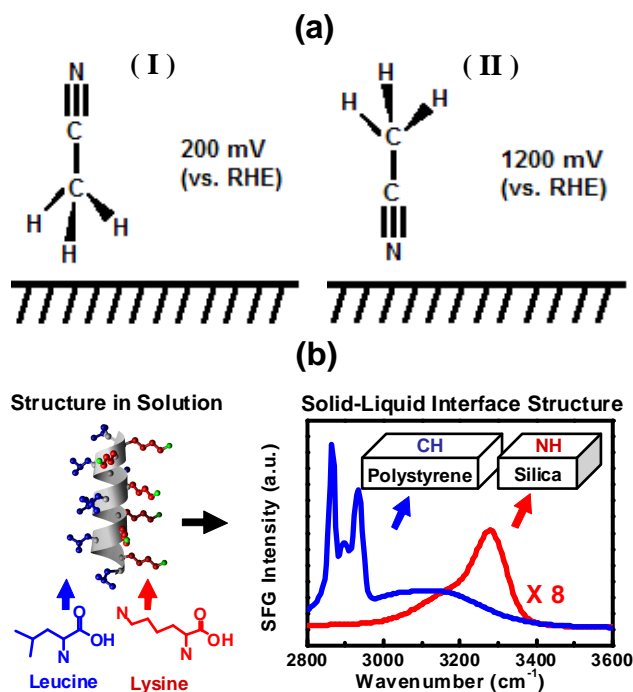
Figure 7. (a) Possible orientations of acetonitrile at Pt (111) electrode. (I) methyl group toward metal (observed at 200 mV with respect to the reference hydrogen electrode (RHE)). (II) Nitrogen lone pair electrons interacting with metal (observed at 1200 mV). (b) SFG spectrum of a 14 amino acid leucine-lysine containing peptide adsorbed onto polystyrene and silica.

VI. Future directions of molecular surface science

Two aspects of future directions in molecular surface science are provided in conclusion. The study of surface science at liquid-solid interfaces is an important task in bridging the pressure gap because the liquid has a thousand times higher density than gas in one atmosphere. We highlight the recent study of the detection of hot electrons generated on the metal thin film or nanoparticles during exothermic catalytic reactions by using a metal-oxide Schottky diode.

VI.a. Surface science at liquid-solid interfaces - surface electrochemistry, and biointerfaces

The ability to monitor the surface structure and orientation of adsorbed molecules with SFG as a function of applied potential is a unique feature of surface electrochemistry. The potential dependent structure of a water/acetonitrile mixture was explored on Pt (111) with SFG. Figure 7a shows the orientation change of acetonitrile as a function of potential of the platinum electrode (52). The CN group is directed toward the metal at potentials where the metal has a positive charge. As the surface becomes less positively charged, the acetonitrile orientation flips 180° with the CH_3 group pointing toward the surface.

From a surface science perspective, the human body may be viewed as a biopolymer-water interface with a layer of adsorbed proteins. Bioimplants, from contact lenses to stents to open arteries and replacements for heart valves, are tools to increase life expectancy and improve quality of life. The challenge is how to make implant materials biocompatible to prevent rejection of artificial replacement organs or devices. Important aspects of biointerface research are studies of the adsorption of proteins and peptides, their surface structure and orientation, which appear to correlate with biocompatibility. These studies are carried out in biologically relevant conditions in aqueous solutions.

Proteins and shorter chain peptides are made up of amino acid molecular building blocks(53). Hydrophobic surfaces that are mostly polymers (such as polystyrene or collagen) or hydrophilic surfaces (such as silica) are used as interfaces most frequently in studies that orient the amino acids in the peptide chains differently. For example, the SFG of a 14 amino acid containing peptide at the hydrophilic (silica/buffer) and hydrophobic (deuterated polystyrene/buffer) interfaces is shown in Fig. 7b. This peptide contains leucine (non-polar) and lysine (polar), amino acids. At the hydrophobic polystyrene interface, the non-polar leucines adsorb and are ordered (and hence seen in the SFG spectra), whereas at the hydrophilic interface, an N-H mode is observed (attributed to the polar lysine side-chains) (54; 55). Hydrogels, which are polymers that adsorb water in large volumes, are an intensive area of biointerface research because of their use in contact lens technology(56).

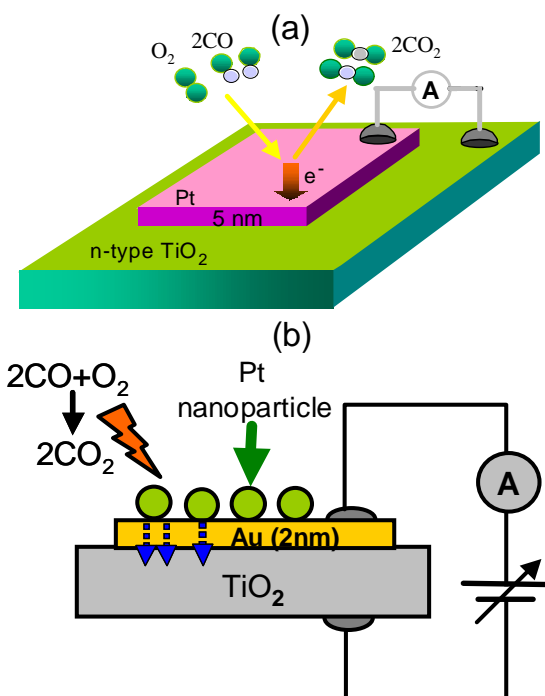**VI.b. Hot electron chemistry – the role of hot electrons in catalytic reactions**

Figure 8. (a) Schematic of hot electron generation in Pt/TiO$_2$ Schottky diode and (b) schematic of hot electron generation in nanoparticles on Au/TiO$_2$ Schottky diode.

One important site for reaction activity and selectivity is the oxide-metal interface, which deserves special attention. It has been known for decades in chemical science and applications that when a metal nanoparticle catalysts is deposited on surfaces of certain oxides that are not chemically active, the reaction rate of the catalyst on a high surface area support is much improved (over ten-fold), as compared to the metal alone. (57; 58) This phenomenon was utilized empirically in catalysis science and the chemical industry by pairing certain oxides with metals to optimize this effect.

The origin of this "strong metal-support interaction" has been attributed to either geometric or electronic effects. The electronic effect involves the generation of hot electrons at metal surfaces that transfer through the metal-oxide interface. During exothermic chemical processes, energetic charge carriers can be generated through non-adiabatic electronic dissipation of chemical energy. Experimental evidences indicating the presence of energetic electrons, known as "hot" electrons, have been reported.

A pulse of energetic photons can generate hot electrons on femtosecond time scales that can be detected by monitoring their kinetic energy in a vacuum, where a large fraction of the photon energy is deposited in the metal. Interestingly, vibrationally excited NO molecules also show very large energy loses (> 1.5 eV) when they are scattered from gold surfaces, while they do not undergo any chemical change. However, the vibrational deexcitation provides energy transfer to the metal that yields hot electrons. As shown by

comparison, lithium fluoride shows no vibrational energy transfer (23) because it has no free electrons.

We constructed a so called catalytic nanodiode(59-61), which is composed of a metal of thickness less than the mean free path of hot electrons, deposited on a semiconductor surface, as shown in Figure 8a. When exothermic catalytic chemical reactions occur, we find that the heat transferred is converted to a hot electron flow that can pass through the metal film into the semiconductor which has a Schottky barrier (62; 63), which allows the passing of energetic electrons in one direction but not in the other direction.

We place the diode into a catalytic reactor and we measure simultaneously the hot electron flow, which is often called "chemicurrent", and the turnover rate. We found that the turnover rate and the chemicurrent are correlated as a function of temperature. The influence of physical and chemical properties of Pt/TiO_2, Pd/TiO_2, and Pt/GaN metal-semiconductor Schottky diodes on the yield of collected hot electron flow (number of hot electrons per product molecule) was investigated(64). It was found that the metal-semiconductor interface structure (roughness, grain size, and step-terrace) is important in controlling the magnitude of the chemicurrent yield.

Recently, we found that hot electrons generated on colloid nanoparticles can be directly detected on Au/TiO_2 diodes(65). The scheme of this device is shown in Figure 8b. The role of Au/TiO_2 diodes is to have a catalytically inactive template diode with a continuous, thin Au layer that ensures that the metal nanoparticles are electrically connected to the device, permitting us to collect hot electrons during exothermic catalytic reactions. Furthermore, the influence of capping layers on the number of hot electrons collected per product molecule generated, also known as the chemicurrent yield, has been investigated. This detection scheme can be used to elucidate the role of the metal-oxide interface in heterogeneous catalysis for practical catalytic systems that involve highly dispersed nanoparticles deposited on an oxide.

The mechanism of how hot electron flows influence catalytic activity is being investigated. This shows the possibility to use hot electron flow to control catalytic activity, while the exothermic catalytic reaction provides the hot electron flow. Hot electron generation can be utilized as a new method for chemical energy conversion.

Acknowledgement

References

[1]   G. Ertl, H.J. Freund, Physics Today 52 (1999) 32-38.
[2]   C.T. Campbell, Surface Science Reports 27 (1997) 1-111.
[3]   H.J. Freund, H. Kuhlenbeck, J. Libuda, G. Rupprechter, M. Baumer, H. Hamann, Topics in Catalysis 15 (2001) 201-209.
[4]   A.T. Bell, Science 299 (2003) 1688-1691.
[5]   G.A. Somorjai, K.M. Bratlie, M.O. Montano, J.Y. Park, Journal of Physical Chemistry B 110 (2006) 20014-20022.
[6]   G.A. Somorjai, J.Y. Park, Catalysis Letters 115 (2007) 87-98.
[7]   G.A. Somorjai, J.Y. Park, Physics Today 60 (2007) 48-53.
[8]   R. Narayanan, M.A. El-Sayed, Nano Letters 4 (2004) 1343-1348.
[9]   J.Y. Park, Y. Zhang, M. Grass, T. Zhang, G.A. Somorjai, Nano Letters 8 (2008) 673 -677.
[10]   G.A. Somorjai, R.L. York, D. Butcher, J.Y. Park, Physical Chemistry Chemical Physics 9 (2007) 3500-3513.
[11]   G.A. Somorjai, A.M. Contreras, M. Montano, R.M. Rioux, Proceedings of the National Academy of Sciences of the United States of America 103 (2006) 10577-10583.
[12]   Woodruff DP, Delchar TA. Modern techniques of surface science. Cambridge: Cambridge University Press; 1986.
[13]   G.A. Somorjai, Introduction to Surface Chemistry and Catalysis, Wiley, New York, (1994).
[14]   M.A. Van Hove, G.A. Somorjai, Journal of Molecular Catalysis a-Chemical 131 (1998) 243-257.
[15]   C.T. Campbell, G. Ertl, H. Kuipers, J. Segner, Surface Science 107 (1981) 220-236.
[16]   X. Bao, J.V. Barth, G. Lehmpfuhl, R. Schuster, Y. Uchida, R. Schlogl, G. Ertl, Surface Science 284 (1993) 14-22.
[17]   U. Schneider, G.R. Castro, K. Wandelt, Surface Science 287 (1993) 146-150.
[18]   K. Wandelt, J. Hulse, J. Kuppers, Surface Science 104 (1981) 212-239.
[19]   M. Salmeron, R.J. Gale, G.A. Somorjai, Journal of Chemical Physics 67 (1977) 5324-5334.
[20]   S. Westerberg, C. Wang, G.A. Somorjai, Surface Science 582 (2005) 137-144.
[21]   N. Toshima, T. Yonezawa, New Journal of Chemistry 22 (1998) 1179-1201.
[22]   J.A. Rodriguez, D.W. Goodman, Science 257 (1992) 897-903.
[23]   Y.H. Huang, C.T. Rettner, D.J. Auerbach, A.M. Wodtke, Science 290 (2000) 111-114.
[24]   A. Bottcher, R. Imbeck, A. Morgante, G. Ertl, Physical Review Letters 65 (1990) 2035-2037.
[25]   D.N. Denzler, C. Frischkorn, C. Hess, M. Wolf, G. Ertl, Physical Review Letters 91 (2003) 226102.
[26]   M. Salmeron, R.J. Gale, G.A. Somorjai, Journal of Chemical Physics 70 (1979) 2807-2818.
[27]   A.L. Marsh, K.A. Becraft, G.A. Somorjai, Journal of Physical Chemistry B 109 (2005) 13619-13622.

[28]   P.S. Cremer, X.C. Su, Y.R. Shen, G.A. Somorjai, Journal of the American Chemical Society 118 (1996) 2942-2949.

[29]   G. Rupprechter, Mrs Bulletin 32 (2007) 1031-1037.

[30]   Y.R. Shen, Nature 337 (1989) 519-525.

[31]   X.C. Su, P.S. Cremer, Y.R. Shen, G.A. Somorjai, Journal of the American Chemical Society 119 (1997) 3994-4000.

[32]   P. Cremer, C. Stanners, J.W. Niemantsverdriet, Y.R. Shen, G. Somorjai, Surface Science 328 (1995) 111-118.

[33]   X.C. Su, P.S. Cremer, Y.R. Shen, G.A. Somorjai, Physical Review Letters 77 (1996) 3858-3860.

[34]   B.L.M. Hendriksen, J.W.M. Frenken, Physical Review Letters 89 (2002).

[35]   J.A. Jensen, K.B. Rider, M. Salmeron, G.A. Somorjai, Physical Review Letters 80 (1998) 1228-1231.

[36]   B.J. McIntyre, M. Salmeron, G.A. Somorjai, Journal of Vacuum Science & Technology a-Vacuum Surfaces and Films 11 (1993) 1964-1968.

[37]   M. Montano, D.C. Tang, G.A. Somorjai, Catalysis Letters 107 (2006) 131-141.

[38]   D.C. Tang, K.S. Hwang, M. Salmeron, G.A. Somorjai, Journal of Physical Chemistry B 108 (2004) 13300-13306.

[39]   M. Montano, K. Bratlie, M. Salmeron, G.A. Somorjai, Journal of the American Chemical Society 128 (2006) 13229-13234.

[40]   K.S. Hwang, M.C. Yang, J. Zhu, J. Grunes, G.A. Somorjai, Journal of Molecular Catalysis a-Chemical 204 (2003) 499-507.

[41]   J. Grunes, J. Zhu, M.C. Yang, G.A. Somorjai, Catalysis Letters 86 (2003) 157-161.

[42]   J. Grunes, J. Zhu, E.A. Anderson, G.A. Somorjai, Journal of Physical Chemistry B 106 (2002) 11463-11468.

[43]   X.M. Yan, S. Kwon, A.M. Contreras, J. Bokor, G.A. Somorjai, Nano Letters 5 (2005) 745-748.

[44]   X.M. Yan, S. Kwon, A.M. Contreras, M.M. Koebel, J. Bokor, G.A. Somorjai, Catalysis Letters 105 (2005) 127-132.

[45]   A.M. Contreras, X.M. Yan, S. Kwon, J. Bokor, G.A. Somorjai, Catalysis Letters 111 (2006) 5-13.

[46]   H. Song, F. Kim, S. Connor, G.A. Somorjai, P.D. Yang, Journal of Physical Chemistry B 109 (2005) 188-193.

[47]   H. Song, R.M. Rioux, J.D. Hoefelmeyer, R. Komor, K. Niesz, M. Grass, P.D. Yang, G.A. Somorjai, Journal of the American Chemical Society 128 (2006) 3027-3037.

[48]   A. Corma, Chemical Reviews 97 (1997) 2373-2419.

[49]   R.M. Rioux, H. Song, J.D. Hoefelmeyer, P. Yang, G.A. Somorjai, Journal of Physical Chemistry B 109 (2005) 2192-2202.

[50]   D. Zhao, P. Yang, N. Melosh, J. Feng, B.F. Chmelka, G.D. Stucky, Advanced Materials 10 (1998) 1380-+.

[51]   K.M. Bratlie, H. Lee, K. Komvopoulos, P. Yang, G.A. Somorjai, Nano Letters 7 (2007) 3097-3101.

[52]   S. Baldelli, G. Mailhot, P.N. Ross, G.A. Somorjai, Journal of the American Chemical Society 123 (2001) 7697-7702.

[53]   J. Kim, G.A. Somorjai, Journal of the American Chemical Society 125 (2003) 3150-3158.

[54]   O. Mermut, D.C. Phillips, R.L. York, K.R. McCrea, R.S. Ward, G.A. Somorjai, Journal of the American Chemical Society 128 (2006) 3598-3607.

[55]   O. Mermut, R.L. York, D.C. Phillips, K.R. McCrea, R.S. Ward, G.A. Somorjai, Biointerphases 1 (2006) P5-P11.

[56]   Q. Chen, D. Zhang, G. Somorjai, C.R. Bertozzi, Journal of the American Chemical Society 121 (1999) 446-447.

[57]   K. Hayek, M. Fuchs, B. Klotzer, W. Reichl, G. Rupprechter, Topics in Catalysis 13 (2000) 55-66.

[58]   A. Boffa, C. Lin, A.T. Bell, G.A. Somorjai, Journal of Catalysis 149 (1994) 149-158.

[59]   X.Z. Ji, A. Zuppero, J.M. Gidwani, G.A. Somorjai, Journal of the American Chemical Society 127 (2005) 5792-5793.

[60]   J.Y. Park, J.R. Renzas, A.M. Contreras, G.A. Somorjai, Topics in Catalysis 46 (2007) 217.

[61]   J.Y. Park, G.A. Somorjai, Chemphyschem 7 (2006) 1409-1413.

[62]   H. Nienhaus, Surface Science Reports 45 (2002) 3-78.

[63]   H. Nienhaus, H.S. Bergh, B. Gergen, A. Majumdar, W.H. Weinberg, E.W. McFarland, Physical Review Letters 82 (1999) 446-449.

[64]   J.Y. Park, J.R. Renzas, B.B. Hsu, G.A. Somorjai, Journal of Physical Chemistry C 111 (2007) 15331-15336.

[65]   J.Y. Park, H. Lee, J.R. Renzas, Y. Zhang, G.A. Somorjai, Nano Letters, DOI: 10.1021/nl8012456 (2008).